

A Convergent Synthetic Approach Using Sterically Demanding Aryldipyrrylmethanes for Tuning the Pocket Sizes of Cofacial Bisporphyrins

Christopher J. Chang,[†] Yongqi Deng,[†] Shie-Ming Peng,[‡] Gene-Hsiang Lee,[‡] Chen-Yu Yeh,[‡] and Daniel G. Nocera^{*,†}

Departments of Chemistry, 6-335, Massachusetts Institute of Technology, 77 Massachusetts Avenue, Cambridge, Massachusetts 02139, and National Taiwan University, Taipei 01764, Taiwan, Republic of China

Received January 15, 2002

Meso substitution opposite to the spacer provides a convenient approach for tuning the pocket sizes of pillared cofacial bisporphyrins. The synthesis and coordination chemistry of xanthene and dibenzofuran anchored platforms structurally modified with 2,6-dimethoxyaryl groups are described. Comparative structural analysis of xanthene derivatives confirms the ability of the *trans*-aryl groups to adjust the vertical dimension of the cofacial cleft: **7** (C₉₇H₁₀₆Cl₄N₈O₅), monoclinic, space group *P*2₁/*c*, *a* = 28.8353(12) Å, *b* = 17.1139(7) Å, *c* = 17.5978(7) Å, β = 98.826(1)°, *Z* = 4; **8** (C₁₀₁H₁₂₃Cl₂N₈O_{11.5}Zn₂), monoclinic, space group *P*2₁/*n*, *a* = 14.5517(6) Å, *b* = 22.9226(10) Å, *c* = 28.5155(13) Å, β = 90.312(14)°, *Z* = 4; **12** (C₉₉H₁₀₂Cl₄N₈O₅Mn₂), monoclinic, space group *P*2₁/*c*, *a* = 19.5891(3) Å, *b* = 15.0741(2) Å, *c* = 33.2019(6) Å, β = 91.947(10)°, *Z* = 4. The convenience and versatility of this synthetic method offers intriguing opportunities to specifically tailor the binding pockets of cofacial bisporphyrins for the study of small-molecule activation within a proton-coupled electron transfer framework.

Introduction

The continuing search for synthetic platforms to catalyze the multielectron transformation of small-molecule substrates has prompted significant attention toward the study of cofacial bisporphyrins and their transition-metal complexes.^{1,2} At the forefront of this research is the development of cofacial “Pacman” bisporphyrins anchored by a single rigid pillar.^{1–13}

Such systems readily provide a face-to-face geometry with little lateral displacement between porphyrin subunits, while the single bridge allows for a range of binding geometries through distortion of the pocket “bite”. For the past 25 years, the cofacial Pacman systems have been limited to two spacers, anthracene (DPA)⁴ and biphenylene (DPB).⁵ These constructs have been quite prominent as electrocatalysts for the reduction of oxygen and other small molecules,^{3–5,10} though the arduous synthesis of their prerequisite dialdehyde bridges has hampered extensive investigation. In addition, the vertical pocket sizes of DPA and DPB bisporphyrins differ by only ca. 1 Å, offering a restricted window of conformational flexibility for exploring structure/function relationships.

Our interest in the activation of small-molecule substrates within a proton-coupled electron transfer framework^{14,15} has

* Author to whom correspondence should be addressed. E-mail: nocera@mit.edu.

[†] Massachusetts Institute of Technology.

[‡] National Taiwan University.

(1) Collman, J. P.; Wagenknecht, P. S.; Hutchinson, J. E. *Angew. Chem., Int. Ed. Engl.* **1994**, *33*, 1537–1554.

(2) Sanders, J. K. M. *Chem. Eur. J.* **1998**, *4*, 1378–1383.

(3) Collman, J. P.; Hutchinson, J. E.; Lopez, M. A.; Tabard, A.; Guillard, R.; Seok, W. K.; Ibers, J. A.; L’Her, M. *J. Am. Chem. Soc.* **1992**, *114*, 9869–9877.

(4) Chang, C. K.; Abdalalmuhdi, I. *J. Org. Chem.* **1983**, *48*, 5388–5390.

(5) Chang, C. K.; Abdalalmuhdi, I. *Angew. Chem., Int. Ed. Engl.* **1984**, *23*, 164–165.

(6) Chang, C. K.; Liu, H. Y.; Abdalalmuhdi, I. *J. Am. Chem. Soc.* **1984**, *106*, 2725–2726.

(7) Lui, H.-Y.; Abdalalmuhdi, I.; Chang, C. K.; Anson, F. C. *J. Phys. Chem.* **1985**, *89*, 665–670.

(8) Ni, C.-L.; Abdalalmuhdi, I.; Chang, C. K.; Anson, F. C. *J. Phys. Chem.* **1987**, *91*, 1158–1166.

(9) Nakash, M.; Clyde-Watson, Z.; Feeder, N.; Davies, J. E.; Teat, S. J.; Sanders, J. K. M. *J. Am. Chem. Soc.* **2000**, *122*, 5286–5293.

(10) Guillard, R.; Lopez, M. A.; Tabard, A.; Richard, P.; Lecomte, C.; Brandes, S.; Hutchinson, J. E.; Collman, J. P. *J. Am. Chem. Soc.* **1992**, *114*, 9877–9889.

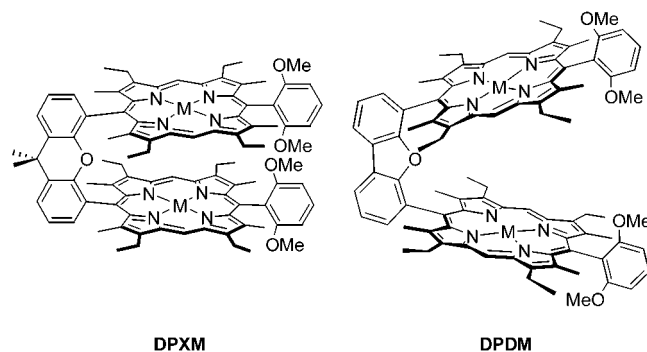
(11) Guillard, R.; Brandes, S.; Tardieux, C.; Tabard, A.; L’Her, M.; Miry, C.; Gouerac, P.; Knop, Y.; Collman, J. P. *J. Am. Chem. Soc.* **1995**, *117*, 11721–11729.

(12) Le Mest, Y.; Inisan, C.; Laouenan, A.; L’Her, M.; Talarmain, J.; El Khalifa, M.; Saillard, J. Y. *J. Am. Chem. Soc.* **1997**, *119*, 6905–6106.

(13) Naruta, Y.; Sasayama, M.; Ichihara, K. *J. Mol. Catal. A* **1997**, *117*, 115–121.

led us to develop new cofacial bisporphyrins supported by xanthene (DPX)¹⁶ and dibenzofuran (DPD) scaffolds.¹⁷ These systems display vertical pocket sizes spanning over 5 Å in metal–metal distances with little to no lateral displacements. In particular, the DPD platform provided the first direct structural evidence for the Pacman effect within a pillared cofacial bisporphyrin motif through a comparative structural analysis of its bizinc(II) and bisiron(III) μ -oxo complexes,¹⁷ which showed that this platform can open and close its binding pocket by a vertical distance of over 4 Å in the presence of appropriate substrates. Moreover, dicobalt(II) complexes of both DPD and DPX are efficient electrocatalysts for the selective four-electron reduction of oxygen to water despite their large difference (ca. 4 Å) in metal–metal distances, demonstrating that the above-mentioned vertical flexibility of these platforms has important ramifications for the dynamic binding, activation, and release of substrates and products.¹⁸

The success of pillared cofacial bisporphyrins for multi-electron small-molecule activation is based on their ability to provide a reaction pocket of suitable size and flexibility. Typically, such structural attributes have been largely controlled by the choice of spacer. In this report, we present a complementary approach for tuning the pocket sizes of pillared bisporphyrins by the selective introduction of sterically demanding aryl groups opposite the cofacial bridge. The synthesis and coordination chemistry of xanthene and dibenzofuran anchored platforms structurally modified with 2,6-dimethoxyaryl groups (DPXM = diporphyrin xanthene methoxyaryl and DPDM = diporphyrin dibenzofuran methoxyaryl, respectively) are described. Crystallographic studies



reveal that the *trans*-aryl groups serve as molecular “teeth” within the cleft of the cofacial bisporphyrin “bite”, affording a powerful approach for systematically tailoring the steric and electronic properties of the binding pockets through minimal changes along the porphyrin superstructure. The versatility of this synthetic methodology opens new avenues

for the development of novel cofacial bisporphyrin systems for proton-coupled small-molecule activation chemistry.

Experimental Section

Materials. Silica gel 60 (70–230 and 230–400 mesh, Fisher) was used for column chromatography. Analytical thin-layer chromatography was performed using silica gel (precoated sheets, 0.2 mm thick). Solvents for synthesis were of reagent grade or better, and were dried according to standard methods.¹⁹ Spectroscopic experiments employed dichloromethane (spectroscopic grade, Burdick & Jackson), which was stored over 4 Å molecular sieves under high vacuum or in a glovebox. Starting materials for syntheses were obtained as follows: 2-(ethyloxycarbonyl)-3-ethyl-4-methylpyrrole (**1**) was obtained from ethyl isocyanoacetate²⁰ and 3-acetoxy-2-nitropentane^{21,22} by the method of Barton and Zard,²³ and 4,5-bis-[4,4'-diethyl-3,3'-dimethyl-2,2'-dipyrrolylmethyl]-9,9-dimethyl-xanthene (**2**)¹⁸ and 4,6-bis[4,4'-diethyl-3,3'-dimethyl-2,2'-dipyrrolylmethyl]dibenzofuran (**3**)¹⁷ were prepared according to previous reports. All other reagents were used as received. Mass spectral analyses were carried out by the University of Illinois Mass Spectrometry Laboratory and the MIT Department of Chemistry Instrument Facility. Elemental analyses were performed at Michigan State University and Quantitative Technologies, Inc. (Whitehouse, New Jersey).

(2,6-Dimethoxyphenyl)bis(5-ethoxycarbonyl-4-ethyl-3-methyl-2-pyrrolyl)methane (4). A mixture of 2,6-dimethoxybenzaldehyde (5.0 g, 30.1 mmol) and **1** (10.9 g, 60.2 mmol, 2 equiv) in absolute ethanol (150 mL) containing concentrated HCl (2.5 mL) was refluxed under nitrogen for 18 h and cooled in an ice bath. The precipitate was filtered and washed with cold methanol to give **4** as a pale-pink powder (13.8 g, 89% yield). ¹H NMR (300 MHz, CDCl₃, 25 °C): δ = 9.07 (br s, 2H, NH), 7.18 (t, J = 8.4 Hz, 1H, ArH), 6.60 (d, J = 8.4 Hz, 2H, ArH), 6.19 (s, 1H, CH), 4.23 (q, J_1 = 7.2 Hz, J_2 = 7.2 Hz, 4H, CH₂), 3.78 (s, 6H, CH₃), 2.69 (q, J_1 = 7.2 Hz, J_2 = 7.5 Hz, 4H, CH₂), 1.81 (s, 6H, CH₃), 1.31 (t, J = 7.2 Hz, 6H, CH₃), 1.06 (t, J = 7.5 Hz, 6H, CH₃).

(2,6-Dimethoxyphenyl)bis(4-ethyl-3-methyl-2-pyrrolyl)methane (5). Powdered NaOH (12 g) in water (15 mL) was combined with **4** (12.0 g, 23.5 mmol) suspended in ethylene glycol (120 mL). The mixture was refluxed under nitrogen for 16 h and cooled to room temperature. The precipitate was collected by suction filtration, washed with water until the washings became neutral, and dried under vacuum over P₂O₅. Product **5**, which was obtained as a goldenrod solid (8.5 g, 99% yield), was stored under nitrogen at –20 °C. ¹H NMR (300 MHz, CDCl₃, 25 °C): δ = 8.15 (br s, 2H, NH), 7.00 (t, J = 8.4 Hz, 1H, ArH), 6.47 (d, J = 8.4 Hz, 2H, ArH), 6.24 (d, J = 2.4 Hz, 2H, CH), 6.07 (s, 1H, CH), 3.63 (s, 6H, CH₃), 2.29 (q, J_1 = 7.5 Hz, J_2 = 7.8 Hz, 4H, CH₂), 1.70 (s, 6H, CH₃), 1.31 (t, J = 7.2 Hz, 6H, CH₃).

(2,6-Dimethoxyphenyl)bis(5-formyl-4-ethyl-3-methyl-2-pyrrolyl)methane (6). Under a nitrogen atmosphere, phosphorus oxychloride (14 mL) was added dropwise to a solution of **5** in anhydrous DMF (50 mL) at –10 °C. After stirring at –10 °C for 30 min, the resulting mixture was allowed to warm to room temperature and stirred for an additional 2 h. The reaction was

- (14) Chang, C. J.; Brown, J. D. K.; Chang, M. C. Y.; Baker, E. A.; Nocera, D. G. In *Electron Transfer in Chemistry*; Balzani, V., Ed.; Wiley-VCH: Weinheim, Germany, 2001; Vol. 3.2.4, pp 409–461.
- (15) Cukier, R. I.; Nocera, D. G. *Annu. Rev. Phys. Chem.* **1998**, *49*, 337–369.
- (16) Chang, C. J.; Deng, Y.; Heyduk, A. F.; Chang, C. K.; Nocera, D. G. *Inorg. Chem.* **2000**, *39*, 959–966.
- (17) Deng, Y.; Chang, C. J.; Nocera, D. G. *J. Am. Chem. Soc.* **2000**, *122*, 410–411.
- (18) Chang, C. J.; Deng, Y.; Shi, C.; Chang, C. K.; Anson, F. C.; Nocera, D. G. *Chem. Commun.* **2000**, 1355–1356.

- (19) Armarego, W. L. F.; Perrin, D. D. *Purification of Laboratory Chemicals*, 4th ed.; Butterworth-Heinemann: Oxford, 1996.
- (20) Harman, G. D.; Wenstock, L. M. *Org. Synth.* **1988**, *VI*, 620–624.
- (21) Tindall, J. B. *Ind. Eng. Chem.* **1941**, *33*, 65–66.
- (22) Sprang, C. A.; Egering, E. F. *J. Am. Chem. Soc.* **1942**, *64*, 1063–1064.
- (23) Barton, D. H. R.; Zard, S. Z. *J. Chem. Soc., Chem. Commun.* **1985**, 1098–1100.

concentrated to half its original volume, and methanol (200 mL) and Na_2CO_3 (20 g) were added. The mixture was heated at 60 °C for 30 min and cooled to room temperature. The precipitate was filtered and washed with water until the washings became neutral. Recrystallization from methanol afforded **6** as an ochre solid (7.2 g, 98% yield). ^1H NMR (300 MHz, CDCl_3 , 25 °C): δ = 9.48 (s, 2H, CHO), 9.14 (br s, 2H, NH), 7.21 (t, J = 8.4 Hz, 1H, ArH), 6.60 (d, J = 8.4 Hz, 2H, ArH), 6.17 (br s, 1H, CH), 3.76 (s, 6H, CH_3), 2.65 (q, J_1 = 7.5 Hz, J_2 = 7.8 Hz, 4H, CH_2), 1.78 (s, 6H, CH_3), 1.15 (t, J = 7.2 Hz, 6H, CH_3).

4,5-Bis[(2,3,13,17-tetraethyl-3,7,12,18-tetramethyl-15-(2,6-dimethoxyphenyl)-5-porphyrinyl)]-9,9-dimethylxanthene, H_4 (DPXM) (7**).** A suspension of **2** (2.19 g, 3.28 mmol) and **6** (2.80 g, 6.63 mmol) in freshly distilled methanol (400 mL) was purged with nitrogen for 20 min. A solution of *p*-toluenesulfonic acid (1.2 g) in methanol (20 mL) was added dropwise over a period of 1 h. The resulting red mixture was stirred in the dark under nitrogen for 2 days. Solid *o*-chloranil (0.9 g) was added in one portion, and stirring was continued in air for 24 h. The mixture was concentrated to half its original volume and the precipitate was suction-filtered and washed with cold methanol and water. The solid was redissolved in chloroform (100 mL), a saturated methanolic solution of $\text{Zn}(\text{OAc})_2 \cdot 2\text{H}_2\text{O}$ (10 mL) was added, and the solution was refluxed for 30 min. The solvent was removed and the remaining residue was purified by flash column chromatography (silica gel, 1:1 dichloromethane/hexanes). The bright red band eluted was collected, taken to dryness, and redissolved in dichloromethane (150 mL). The solution was vigorously stirred with 6 N HCl (16 mL) for 15 min and neutralized with a 10% aqueous sodium carbonate solution, and the mixture was stirred for an additional 15 min. The organic phase was separated, washed with water (3×50 mL), dried over Na_2SO_4 , and taken to dryness. Recrystallization from dichloromethane/methanol afforded pure **7** as a royal purple microcrystalline powder (1.57 g, 34% yield). ^1H NMR (500 MHz, CDCl_3 , 25 °C): δ = 8.01 (s, 4H, meso), 7.95 (d, J = 9.9 Hz, 2H, ArH), 7.76 (t, J = 8.4 Hz, 2H, ArH), 7.28 (t, J = 7.5 Hz, 2H, ArH), 7.19 (d, J = 8.7 Hz, 2H, ArH), 6.98 (d, J = 7.2 Hz, 2H, ArH), 6.80 (d, J = 8.7 Hz, 2H, ArH), 4.17 (s, 6H, OCH_3), 3.33 (m, 4H, CH_2), 3.02 (s, 6H, OCH_3), 2.70 (m, 4H, CH_2), 2.53 (s, 12H, CH_3), 2.33 (s, 6H, CH_3), 2.25 (s, 12H, CH_3), 1.70 (m, 4H, CH_2), 1.28 (t, J = 7.2 Hz, 6H, CH_3), 0.729 (t, J = 7.2 Hz, 6H, CH_3), -2.27 (br s, 2H, NH), -3.68 (br s, 2H, NH). HRFABMS (MH^+) calcd for $\text{C}_{95}\text{H}_{102}\text{N}_8\text{O}_5$ m/z 1435.798, found 1435.804.

Zn_2 (DPXM) (8**).** A saturated methanolic solution of $\text{Zn}(\text{OAc})_2 \cdot 2\text{H}_2\text{O}$ (1 mL) was added to a solution of **7** (20 mg, 0.014 mmol) in chloroform (5 mL). The reaction was refluxed for 30 min and taken to dryness. The solid residue was purified by flash column chromatography (silica gel, 1:1 to 3:1 dichloromethane/hexanes) followed by recrystallization from dichloromethane/methanol to deliver analytically pure **8** as a scarlet microcrystalline powder in essentially quantitative yield. ^1H NMR (500 MHz, CDCl_3 , 25 °C): δ = 8.40 (s, 4H, meso), 7.83 (d, J = 7.8 Hz, 2H, ArH), 7.50 (t, J = 8.4 Hz, 2H, ArH), 7.12 (t, J = 6.9 Hz, 2H, ArH), 6.88 (d, J = 8.4 Hz, 2H, ArH), 6.73 (d, J = 6.9 Hz, 2H, ArH), 6.63 (d, J = 8.4 Hz, 2H, ArH), 3.63 (s, 6H, OCH_3), 3.35 (m, 4H, CH_2), 3.07 (m, 8H, CH_2), 2.88 (s, 6H, OCH_3), 2.71 (m, 4H, CH_2), 2.33 (s, 6H, CH_3), 2.23 (s, 24H, CH_3), 1.24 (t, J = 7.2 Hz, 6H, CH_3), 1.06 (t, J = 7.2 Hz, 6H, CH_3). Anal. Calcd for $\text{C}_{95}\text{H}_{98}\text{N}_8\text{O}_5\text{Zn}_2$: C, 73.02; H, 6.32; N, 7.17. Found: C, 73.06; H, 6.56; N, 7.17. HRFABMS (M^+): calcd for $\text{C}_{95}\text{H}_{98}\text{N}_8\text{O}_5\text{Zn}_2$ m/z 1558.624, found 1558.630.

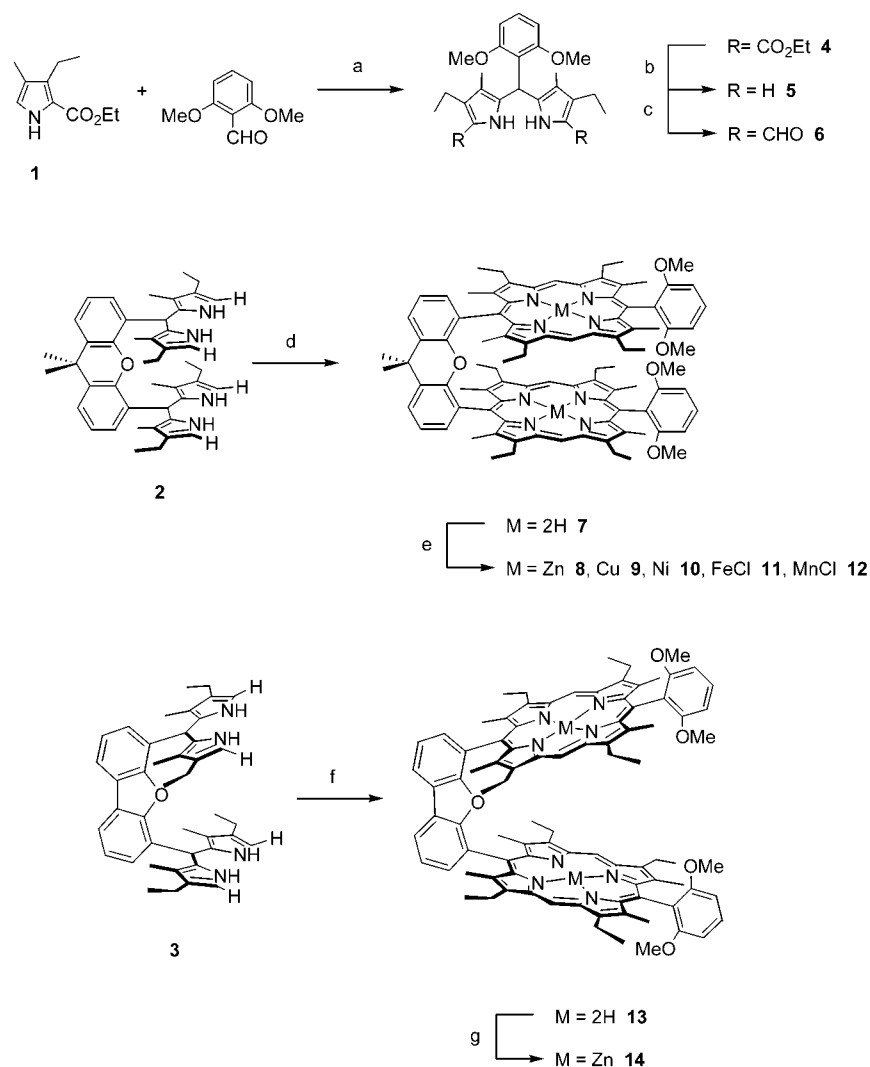
Cu_2 (DPXM) (9**).** To a 12-mL chloroform solution of **7** (56 mg, 0.039 mmol) was added a solution of $\text{Cu}(\text{OAc})_2 \cdot 2\text{H}_2\text{O}$ (130 mg) and potassium acetate (145 mg) in 12 mL of methanol. The resulting

solution was refluxed for 5 h, and the solvent was removed by rotary evaporation. The remaining solid was taken up in a 1:1 mixture of dichloromethane/water (150 mL). The organic layer was decanted and taken to dryness. The crude material was purified by flash column chromatography (silica gel, 1:1 dichloromethane/hexanes) followed by recrystallization from dichloromethane/methanol to afford analytically pure **9** as a brick red solid (53 mg, 87% yield). Anal. Calcd for $\text{C}_{95}\text{H}_{98}\text{N}_8\text{O}_5\text{Cu}_2$: C, 73.19; H, 6.34; N, 7.19. Found: C, 73.05; H, 6.24; N, 7.14. HRFABMS (M^+): calcd for $\text{C}_{95}\text{H}_{98}\text{N}_8\text{O}_5\text{Cu}_2$ m/z 1556.645, found 1556.644.

Ni_2 (DPXM) (10**).** A mixture of **7** (53 mg, 0.037 mmol) and NiCl_2 (102 mg, mmol) in 6 mL of DMF was refluxed under nitrogen for 4 h. The solvent was removed under vacuum, and the remaining solid was taken up in a 1:1 mixture of dichloromethane/water (150 mL). The organic layer was decanted and taken to dryness. Purification by flash column chromatography (silica gel, 1:1 dichloromethane/hexanes) followed by recrystallization from dichloromethane/methanol gave analytically pure **10** as a ruby red microcrystalline powder (46 mg, 81% yield). ^1H NMR (500 MHz, CDCl_3 , 25 °C): δ = 7.83 (d, 2H, ArH), 7.76 (s, 4H, meso), 7.58 (t, J = 7.5 Hz, 2H, ArH), 7.16 (t, J = 7.8 Hz, 2H, ArH), 7.04 (d, J = 8.7 Hz, 2H, ArH), 6.82 (d, J = 7.2 Hz, 2H, ArH), 6.68 (d, J = 8.4 Hz, 2H, ArH), 4.11 (s, 6H, OCH_3), 3.03 (s, 6H, OCH_3), 2.72 (m, 4H, CH_2), 2.50 (m, 4H, CH_2), 2.24 (m, 8H, CH_2), 2.21 (s, 6H, CH_3), 2.17 (s, 12H, CH_3), 2.12 (s, 12H, CH_3), 1.15 (t, J = 7.2 Hz, 6H, CH_3), 1.03 (t, J = 7.2 Hz, 6H, CH_3). Anal. Calcd for $\text{C}_{95}\text{H}_{98}\text{N}_8\text{O}_5\text{Ni}_2$: C, 73.65; H, 6.38; N, 7.23. Found: C, 73.53; H, 6.22; N, 7.42. HRFABMS (M^+): calcd for $\text{C}_{95}\text{H}_{98}\text{N}_8\text{O}_5\text{Ni}_2$ m/z 1546.637, found 1546.636.

Fe_2Cl_2 (DPXM) (11**).** In a drybox, a 100-mL flask equipped with a condenser was charged with **7** (202 mg, 0.141 mmol), 2,6-lutidine (0.4 mL), FeBr_2 (495 mg), THF (25 mL), and benzene (12 mL). The mixture was refluxed under nitrogen for 12 h, opened to air, and brought to dryness under vacuum. The residue was taken up in a 1:1 mixture of dichloromethane/water (50 mL). The organic layer was separated, washed with water (3×75 mL), and stirred with a 5:1 mixture of saturated aqueous NaCl and HCl (72 mL) for 90 min. The organic layer was decanted, and solvent was removed under vacuum. The remaining solid was purified by column chromatography (silica gel, dichloromethane to 5% methanol/dichloromethane) and retreated with aqueous NaCl and HCl as described above. The organic phase was separated, washed with water (3×75 mL), dried over Na_2SO_4 , and taken to dryness. Recrystallization from dichloromethane and ether afforded pure **11** as a brown powder (189 mg, 83% yield). Anal. Calcd for $\text{C}_{95}\text{H}_{98}\text{N}_8\text{O}_5\text{Cl}_2\text{Fe}_2$: C, 70.68; H, 6.12; N, 6.94. Found: C, 70.72; H, 6.15; N, 7.00. HRFABMS ($[\text{M} - \text{Cl}]^+$): calcd for $\text{C}_{95}\text{H}_{98}\text{N}_8\text{O}_5\text{Cl}_2\text{Fe}_2$ m/z 1577.605, found 1577.599.

Mn_2Cl_2 (DPXM) (12**).** A solution of **7** (202 mg, 0.141 mmol) and $\text{Mn}(\text{OAc})_2 \cdot 4\text{H}_2\text{O}$ (495 mg) in DMF (15 mL) was refluxed in air for 3 h. The reaction was cooled to room temperature and taken to dryness. The residue was taken up in a 1:1 mixture of dichloromethane/water (50 mL). The organic layer was separated, washed with water (3×75 mL), and stirred with a 5:1 mixture of saturated aqueous NaCl and HCl (72 mL) for 90 min. The organic layer was decanted and solvent was removed under vacuum. The remaining solid was purified by column chromatography (silica gel, dichloromethane to 5% methanol/dichloromethane) and retreated with aqueous NaCl and HCl as described above. The organic phase was separated, washed with water (3×75 mL), dried over Na_2SO_4 , and taken to dryness. Recrystallization from dichloromethane and ether afforded pure **12** as a brown solid (202 mg, 89% yield). Anal. Calcd for $\text{C}_{95}\text{H}_{98}\text{N}_8\text{O}_5\text{Cl}_2\text{Mn}_2$: C, 70.76; H, 6.13; N, 6.95;

Scheme 1^a

^a (a) Ethanol, HCl, reflux; (b) NaOH, ethylene glycol, reflux; (c) (i) POCl₃/DMF; (ii) Na₂CO₃; (d) (i) **6**, *p*-TsOH, methanol; (ii) *o*-chloranil; (e) MX₂, reflux. (f) (i) **6**, *p*-TsOH, methanol; (ii) *o*-chloranil; (g) Zn(OAc)₂·2H₂O, chloroform/methanol, reflux.

Cl, 4.40. Found: C, 70.35; H, 6.56; N, 6.84; Cl, 4.40. HRFABMS ([M – Cl]⁺): calcd for C₉₅H₉₈N₈O₅Cl₂Mn₂ *m/z* 1575.611, found 1575.611.

4,6-Bis[(2,3,13,17-tetraethyl-3,7,12,18-tetramethyl-15-(2,6-dimethoxyphenyl)-5-porphyrinyl)]-dibenzofuran, H₄(DPDM) (13**).** A suspension of **3** (1 g, 1.60 mmol) and **6** (2.8 g, 3.20 mmol) in freshly distilled methanol (300 mL) was purged with nitrogen for 15 min. A solution of *p*-toluenesulfonic acid (0.67 g) in methanol (15 mL) was added dropwise over a period of 90 min. The resulting red mixture was stirred in the dark under nitrogen for 2 days. Solid *o*-chloranil (533 mg) was added in one portion, and stirring was continued in air for 24 h. The mixture was taken to dryness, and the solid was redissolved in chloroform (50 mL). A saturated methanolic solution of Zn(OAc)₂·2H₂O (5 mL) was added, and the solution was refluxed for 1 h. The solvent was removed and the remaining residue was purified by repeated flash column chromatography (silica gel, 1:1 dichloromethane/hexanes). The bright red band that eluted was collected, taken to dryness, and redissolved in dichloromethane (60 mL). The solution was vigorously stirred with 6 N HCl (6 mL) for 25 min. The solution was neutralized with a 10% aqueous sodium carbonate solution, and the mixture was stirred for an additional 15 min. The organic phase was

separated, washed with water (3 × 25 mL), dried over Na₂SO₄, and taken to dryness. Recrystallization from dichloromethane/methanol afforded pure **13** as a plum solid (250 mg, 11% yield). ¹H NMR (500 MHz, CDCl₃, 25 °C): δ = 9.78 (s, 4H, meso), 8.66 (d, *J* = 7.5 Hz, 2H, ArH), 7.76 (t, *J* = 6.9 Hz, 2H, ArH), 7.70 (d, *J* = 7.2 Hz, 2H, ArH), 7.58 (t, *J* = 7.8 Hz, 2H, ArH), 6.83 (d, *J* = 8.2 Hz, 2H, ArH), 6.80 (d, *J* = 8.2 Hz, 2H, ArH), 3.80 (m, 16H, CH₂), 3.37 (s, 6H, OCH₃), 3.17 (s, 6H, OCH₃), 2.43 (s, 12H, CH₃), 2.36 (s, 12H, CH₃), 1.58 (m, 24H, CH₃), –2.83 (br s, 4H, NH). HRFABMS (M⁺): calcd for C₉₂H₉₆N₈O₅ *m/z* 1393.798, found 1393.758.

Zn₂(DPDM) (14**).** A saturated methanolic solution of Zn(OAc)₂·2H₂O (1 mL) was added to a solution of **13** (50 mg, 0.0359 mmol) in chloroform (5 mL). The reaction mixture was refluxed for 30 min and taken to dryness. The solid residue was purified by flash column chromatography (silica gel, 3:1 dichloromethane/hexanes) followed by recrystallization from dichloromethane/methanol to deliver analytically pure **14** as a bright red powder in essentially quantitative yield. ¹H NMR (500 MHz, CDCl₃, 25 °C): δ = 9.72 (s, 4H, meso), 8.65 (d, *J* = 7.5 Hz, 2H, ArH), 7.74 (m, 4H, ArH), 7.58 (t, *J* = 8.1 Hz, 2H, ArH), 6.85 (d, *J* = 7.8 Hz, 2H, ArH), 6.79 (d, *J* = 8.4 Hz, 2H, ArH), 3.77 (m, 16H, CH₂), 3.41 (s, 6H, OCH₃),

3.09 (s, 6H, OCH₃), 2.43 (s, 12H, CH₃), 2.34 (s, 12H, CH₃), 1.59 (m, 24H, CH₃). Anal. Calcd for C₉₂H₉₂N₈O₅Zn₂: C, 72.67; H, 6.10; N, 7.37. Found: C, 72.44; H, 5.84; N, 7.49. HRFABMS (M⁺): calcd for C₉₅H₉₈N₈O₅Zn₂ *m/z* 1516.577, found 1516.567.

General Details of X-ray Data Collection and Reduction.

X-ray diffraction data were collected using a Siemens three-circle diffractometer equipped with a CCD detector. Measurements were carried out at $-90\text{ }^{\circ}\text{C}$ using Mo K α ($\lambda = 0.71073\text{ \AA}$) radiation, which was wavelength selected with a single-crystal graphite monochromator. Four sets of data were collected using ω scans and a -0.3° scan width. All calculations were performed using a PC workstation. The data frames were integrated to *hkl*/intensity, and final unit cells were calculated by using the SAINT v.4.050 program from Siemens. The structures were solved and refined with the SHELXTL v.5.03 suite of programs developed by G. M. Sheldrick and Siemens Industrial Automation, Inc., 1995.

X-ray Structure of H₄(DPXM)·2CH₂Cl₂ (7). A 0.50 mm \times 0.31 mm \times 0.30 mm royal purple crystal of plate morphology was obtained from slow diffusion of methanol into a dichloromethane solution of the compound. The crystal was coated in STP and mounted onto a glass fiber. A total of 43593 reflections were collected in the θ range $2.14\text{--}26.37^{\circ}$, of which 17101 were unique ($R_{\text{int}} = 0.0342$). Hydrogen atoms were placed in calculated positions using a standard riding model and were refined isotropically. The largest peak and hole in the difference map were 0.934 and -0.502 e \AA^{-3} , respectively. The least squares refinement converged normally, giving residuals of $R1 = 0.0683$ and $wR2 = 0.1850$, with $\text{GOF} = 1.051$.

X-ray Structure of Zn₂(DPXM)·5CH₃OH·1.5H₂O·CH₂Cl₂ (8). A 0.10 mm \times 0.26 mm \times 0.40 mm brick red crystal of needle morphology was obtained from slow diffusion of methanol into a dichloromethane solution of the compound. The crystal was coated in STP and mounted onto a glass fiber. A total of 48278 reflections were collected in the θ range $2.32\text{--}26.38^{\circ}$, of which 19020 were unique ($R_{\text{int}} = 0.0394$). The Patterson method was used to locate the zinc atoms; all remaining atoms were placed using the difference Fourier map. Hydrogen atoms were placed in calculated positions using a standard riding model and were refined isotropically. A disordered ethyl group attached to C(28) was assigned half-occupancy in two different conformations. Oxygen atoms O(8) and O(11) from two disordered methanol solvent molecules were assigned half-occupancy in two different conformations. The largest peak and hole in the difference map were 1.208 and -0.931 e \AA^{-3} , respectively. The least squares refinement converged normally, giving residuals of $R1 = 0.0854$ and $wR2 = 0.2323$, with $\text{GOF} = 1.022$.

X-ray Structure of Mn₂Cl₂(DPXM)·4CHCl₃ (12). A 0.50 mm \times 0.25 mm \times 0.20 mm dark brown crystal of needle morphology was obtained from slow diffusion of hexane into a chloroform solution of the compound. The crystal was coated in STP and mounted onto a glass fiber. A total of 38526 reflections were collected in the θ range $1.23\text{--}23.24^{\circ}$, of which 14012 were unique ($R_{\text{int}} = 0.0446$). The Patterson method was used to locate the manganese atoms; all remaining atoms were placed using the difference Fourier map. Hydrogen atoms were placed in calculated positions using a standard riding model and were refined isotropically. The largest peak and hole in the difference map were 1.486 and -1.021 e \AA^{-3} , respectively. The least squares refinement converged normally, giving residuals of $R1 = 0.0812$ and $wR2 = 0.2045$, with $\text{GOF} = 1.101$.

Physical Measurements. ¹H NMR spectra were collected in CDCl₃ (Cambridge Isotope Laboratories) at the MIT Department of Chemistry Instrumentation Facility (DCIF) using either a Unity

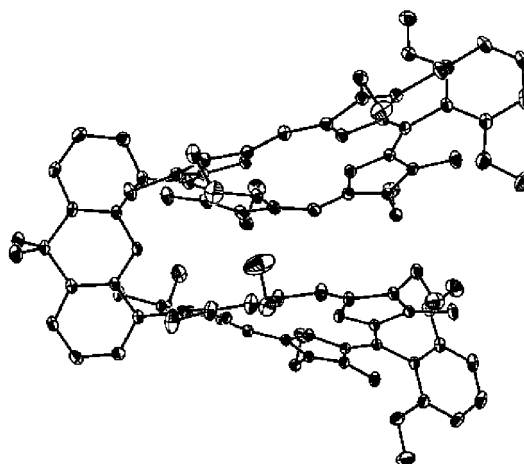


Figure 1. Crystal structure of H₄(DPXM) (7). Thermal ellipsoids are drawn at the 25% probability level. Hydrogen atoms and solvent molecules within the lattice have been omitted for clarity.

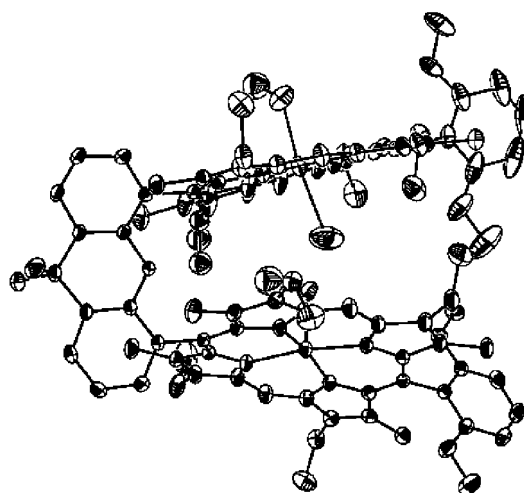


Figure 2. Crystal structure of Zn₂(DPXM) (8). Thermal ellipsoids are drawn at the 25% probability level. Hydrogen atoms and solvent molecules within the lattice have been omitted for clarity.

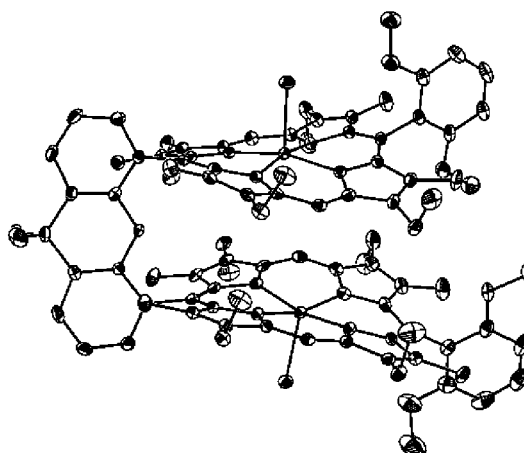


Figure 3. Crystal structure of Mn₂Cl₂(DPXM) (12). Thermal ellipsoids are drawn at the 25% probability level. Hydrogen atoms and solvent molecules within the lattice have been omitted for clarity.

300, Mercury 300, or Inova 500 spectrometer at $25\text{ }^{\circ}\text{C}$. All chemical shifts are reported using the standard δ notation in parts per million; positive chemical shifts are to higher frequency from the given reference. Absorption spectra were obtained using a Cary-17

Table 1. Crystallographic Data for **7**, **8**, and **12**

	7	8	12
empirical formula	C ₉₇ H ₁₀₆ Cl ₄ N ₈ O ₅	C ₁₀₁ H ₁₂₃ Cl ₂ N ₈ O _{11.5} Zn ₂	C ₉₉ H ₁₀₂ Cl ₁₄ N ₈ O ₅ Mn ₂
fw	1605.72	1834.71	2090.10
<i>T</i> (K)	183(2)	183(2)	183(2)
λ (Å)	0.71073	0.71073	0.71073
cryst syst	monoclinic	monoclinic	monoclinic
space group	<i>P</i> 2 ₁ / <i>c</i>	<i>P</i> 2 ₁ / <i>n</i>	<i>P</i> 2/ <i>c</i>
<i>a</i> (Å)	28.8353(12)	14.5517(6)	19.5891(3)
<i>b</i> (Å)	17.1139(7)	22.9226(10)	15.0741(2)
<i>c</i> (Å)	17.5978(7)	28.5155(13)	33.2019(6)
α (deg)	90	90	90
β (deg)	98.826(1)	90.3121(14)	91.947(10)
γ (deg)	90	90	90
<i>V</i> (Å ³)	8581.4(6)	9511.6(7)	9798.5(3)
<i>Z</i>	4	4	4
ρ_{calcd} (g cm ⁻³)	1.243	1.281	1.420
abs coeff (mm ⁻¹)	0.196	0.624	0.696
<i>F</i> (000)	3408	3884	4336
reflns collcd	43593	48278	38526
ind reflns	17101 (<i>R</i> _{int} = 0.0342)	19020 (<i>R</i> _{int} = 0.0394)	14012 (<i>R</i> _{int} = 0.0446)
max/min transm	0.9828/0.8316	0.8944/0.6748	0.2752/0.2252
data/restraints/params	17101/0/1043	19020/4/1078	13991/0/1154
GOF ^b on <i>F</i> ²	1.051	1.022	1.101
<i>R</i> 1 ^a (<i>F</i> _o ²) (>2 σ (<i>I</i>))	0.0683	0.0854	0.0812
	w <i>R</i> 2 ^b = 0.19	w <i>R</i> 2 ^b = 0.1994	w <i>R</i> 2 ^b = 0.1460
<i>R</i> 1 ^a (<i>F</i> _o ²) (all data)	0.0833	0.1283	0.1026

^a *R*1 = $\sum||F_o| - |F_c||/\sum|F_o|$. ^b GOF = $(\sum w(F_o^2 - F_c^2)^2/(n - p))^{1/2}$ where *n* is the number of data and *p* is the number of parameters refined.

spectrophotometer modified by On-Line Instrument Systems (OLIS) to include computer control or a Spectral Instruments 440 spectrophotometer.

Results and Discussion

Synthesis. The synthetic strategy for the preparation of pillared cofacial bisporphyrins containing a single aryl group *trans* to the spacer is outlined in Scheme 1. We employ the convergent three-branch approach developed by Chang⁴ and modified by Collman;³ the stepwise approach described here allows for the synthesis of meso and/or β -substituted derivatives with more precise control over statistical methods (e.g., Adler–Longo, Lindsey) that have been previously used to prepare β -free cofacial bisporphyrins bearing meso-aryl substituents.^{24,25}

Aryl-substituted dipyrromethane dialdehydes are conveniently supplied in a three-step protocol from a pyrrole and an aldehyde; the 2,6-dimethoxyphenyl derivative is an exemplary system. Ester-protected dipyrromethane **4** is obtained in 89% yield by acid-catalyzed reaction of 2,6-dimethoxybenzaldehyde with pyrrole **1** in boiling ethanol. Deprotection of the α -ethyl esters of **4** with sodium hydroxide in ethylene glycol gives α -free dipyrromethane **5** in almost quantitative yield. Vilsmeier formylation of **5** using POCl₃/DMF followed by base hydrolysis produces **6** in 98% yield.

Cyclization of xanthene tetrapyrrole **2** with **6** in the presence of *p*-toluenesulfonic acid (PTSA) followed by oxidation with *o*-chloranil affords bisporphyrin **7** (DPXM = diporphyrin xanthene methoxyaryl) after workup and purification. The yield for the final coupling step (34%) is

Table 2. Selected Geometric Lengths (Å) for **7**, **8**, and **12**

	7	8	12
Ct(1)–N(1)	2.129	Zn(1)–N(1) 2.063(4)	Mn(1)–N(1) 2.015(5)
Ct(1)–N(2)	2.014	Zn(1)–N(2) 2.062(4)	Mn(1)–N(2) 1.999(5)
Ct(1)–N(3)	2.118	Zn(1)–N(3) 2.066(4)	Mn(1)–N(3) 2.015(5)
Ct(1)–N(4)	2.021	Zn(1)–N(4) 2.057(4)	Mn(1)–N(4) 1.996(5)
Ct(2)–N(5)	2.013	Zn(2)–N(5) 2.047(4)	Mn(2)–N(5) 2.004(7)
Ct(2)–N(6)	2.119	Zn(2)–N(6) 2.049(5)	Mn(2)–N(6) 2.014(5)
Ct(2)–N(7)	2.007	Zn(2)–N(7) 2.065(4)	Mn(2)–N(7) 2.010(4)
Ct(2)–N(8)	2.114	Zn(2)–N(8) 2.068(4)	Mn(2)–N(8) 2.017(5)
O(1)–C(52)	1.375(3)	Zn(1)–O(6) 2.175(5)	Mn(1)–Cl(8) 2.400(2)
O(1)–C(53)	1.376(3)	Zn(2)–O(7) 2.252(6)	Mn(2)–Cl(2) 2.409(2)
		Zn(2)–O(8) 2.459(17)	

the highest reported for these types of pillared compounds. The ¹H NMR spectrum of **7** is consistent with a splayed structure in solution, as the internal NH-pyrrolic resonances (δ –2.27, –3.68 ppm) are in the same range as an analogous monomeric xanthene porphyrin (δ –3.10, –3.29 ppm).¹⁶

Homobimetallic coordination complexes of **7** are prepared smoothly by direct reaction with metal salts. The binuclear zinc(II) complex Zn₂(DPXM) (**8**) is obtained in quantitative yield by reaction of **7** with Zn(OAc)₂·2H₂O in methanol/chloroform mixtures. Complex **8** was characterized by ¹H NMR, high-resolution mass spectrometry, and elemental analyses. The biscopper(II) complex Cu₂(DPXM) (**9**) is prepared in excellent yield (87%) using Cu(OAc)₂·2H₂O and potassium acetate in methanol/chloroform mixtures. Complex **9** gave satisfactory mass spectral and elemental analyses. Dinickel complex Ni₂(DPXM) (**10**) is synthesized in good yield (81%) using Adler's method (NiCl₂/DMF). The diamagnetic compound was characterized by ¹H NMR, high-resolution mass spectrometry, and elemental analyses. Bis-chloroiron(III) compound **11** is delivered in good yield (83%) from FeBr₂ and 2,6-lutidine in a THF/benzene solvent system followed by anion exchange with aqueous NaCl and HCl. Satisfactory high-resolution mass spectral data and elemental

(24) Collman, J. P.; Tyvoll, D. A.; Chng, L. L.; Fish, H. T. *J. Org. Chem.* **1995**, *60*, 1926–1931.

(25) Naruta, Y.; Sasayama, M. *J. Chem. Soc., Chem. Commun.* **1994**, 2667–2668.

Table 3. Selected Geometric Angles (deg) for **7**, **8** and **12**

7		8		12	
N(1)–Ct(1)–N(2)	83.3	N(1)–Zn(1)–N(2)	86.6(2)	N(1)–Mn(1)–N(2)	91.9(2)
N(1)–Ct(1)–N(3)	179.4	N(1)–Zn(1)–N(3)	166.3(2)	N(1)–Mn(1)–N(3)	163.1(2)
N(2)–Ct(1)–N(3)	96.5	N(2)–Zn(1)–N(3)	92.0(2)	N(2)–Mn(1)–N(3)	86.4(2)
N(1)–Ct(1)–N(4)	97.0	N(1)–Zn(1)–N(4)	92.1(2)	N(1)–Mn(1)–N(4)	86.6(2)
N(2)–Ct(1)–N(4)	179.3	N(2)–Zn(1)–N(4)	169.9(2)	N(2)–Mn(1)–N(4)	168.3(2)
N(3)–Ct(1)–N(4)	83.2	N(3)–Zn(1)–N(4)	86.9(2)	N(3)–Mn(1)–N(4)	91.7(2)
N(7)–Ct(2)–N(8)	83.4	N(7)–Zn(2)–N(8)	86.5(2)	N(7)–Mn(2)–N(8)	92.4(2)
N(7)–Ct(2)–N(6)	96.5	N(7)–Zn(2)–N(6)	92.5(2)	N(7)–Mn(2)–N(6)	85.3(2)
N(8)–Ct(2)–N(6)	177.8	N(8)–Zn(2)–N(6)	172.0(2)	N(8)–Mn(2)–N(6)	162.2(2)
N(7)–Ct(2)–N(5)	177.7	N(7)–Zn(2)–N(5)	176.1(2)	N(7)–Mn(2)–N(5)	166.6(2)
N(8)–Ct(2)–N(5)	96.5	N(8)–Zn(2)–N(5)	92.8(2)	N(8)–Mn(2)–N(5)	86.3(2)
N(6)–Ct(2)–N(5)	83.7	N(6)–Zn(2)–N(5)	87.7(2)	N(6)–Mn(2)–N(5)	91.9(2)
C(53)–O(1)–C(52)	119.6(2)	N(1)–Zn(1)–O(6)	99.2(2)	N(1)–Mn(1)–Cl(1)	98.2(1)
C(52)–C(51)–C(25)	121.3(2)	N(2)–Zn(1)–O(6)	94.6(2)	N(2)–Mn(1)–Cl(1)	94.3(2)
C(53)–C(41)–C(5)	122.3(2)	N(3)–Zn(1)–O(6)	94.5(2)	N(3)–Mn(1)–Cl(1)	98.7(1)
C(50)–C(51)–C(25)	120.0(2)	N(4)–Zn(1)–O(6)	95.5(2)	N(4)–Mn(1)–Cl(1)	97.4(1)
C(42)–C(41)–C(5)	119.3(2)	N(5)–Zn(2)–O(7)	94.2(2)	N(5)–Mn(2)–Cl(2)	97.1(1)
C(51)–C(52)–O(1)	115.0(2)	N(6)–Zn(2)–O(7)	92.5(2)	N(6)–Mn(2)–Cl(2)	102.6(2)
C(41)–C(53)–O(1)	115.0(2)	N(7)–Zn(2)–O(7)	89.7(2)	N(7)–Mn(2)–Cl(2)	96.3(1)
		N(8)–Zn(2)–O(7)	83.6(5)	N(8)–Mn(2)–Cl(2)	95.2(1)

analyses accompanied **11**. Lastly, bischloromanganese(III) complex **12** is afforded in high yield (89%) by an Adler reaction of **7** with $\text{Mn}(\text{OAc})_2 \cdot 4\text{H}_2\text{O}$ in DMF with subsequent anion exchange in the same manner as the bischloroiron-(III) derivative (aqueous NaCl/HCl).

The use of dipyrromethane dialdehyde **6** is not limited to bisporphyrin templates containing a xanthene pillar. For example, the dibenzofuran tetrapyrrole undergoes cyclization with **6** in the presence of PTSA to give the corresponding cofacial bisporphyrin $\text{H}_4(\text{DPDM})$ (**13**) (DPDM = diporphyrin dibenzofuran methoxyaryl) in 11% yield. As observed for **7** and the parent bisporphyrin $\text{H}_4(\text{DPD})$, the chemical shift for the internal NH-pyrrolic resonances (δ –2.83 ppm) indicates an open structure in solution.¹⁷ Zinc insertion proceeds in quantitative yield using the standard method ($\text{Zn}(\text{OAc})_2 \cdot 2\text{H}_2\text{O}$, methanol/dichloromethane) to generate $\text{Zn}_2(\text{DPDM})$ (**14**). Complex **14** was fully characterized by ^1H NMR, high-resolution spectrometry, and elemental analyses.

Structural Chemistry. The structural consequences of a single aryl group *trans* to the spacer have been investigated using single-crystal X-ray analysis. In order to provide a systematic study, three structures of the DPXM framework have been determined for comparison with known DPX and DPD congeners: the free-base bisporphyrin **7**, compound **8** containing the non-redox-active zinc(II) metal, and complex **12** bearing redox-active manganese centers.

The molecular structures of **7**, **8**, and **12** are shown in Figures 1–3, respectively. Crystallographic data and selected geometrical measurements are given in Tables 1–4. Trends in bond lengths and angles of macrocyclic core structures and side chains agree well with those observed in related systems such as $\text{H}_4(\text{DPX})$, $\text{H}_4(\text{DPD})$, $\text{H}_4(\text{DPA})$, and $\text{H}_4(\text{DPB})$.^{1,3,9–11,16–18,26–29} Structural highlights of the core structures for **7**, **8**, and **12** are as follows:

Table 4. Crystallographically Derived Intradimer Geometrical Features for DPX, DPD, and DPXM Compounds^a

	M–M (Å)	Ct–Ct (Å)	inter- planar angle (deg)	torsional twist (deg)	a–b dist (Å)	c–d dist (Å)
$\text{H}_4(\text{DPX})$ ³⁰	na	4.002	4.7	14.3	3.552	4.324
$\text{H}_4(\text{DPD})$ ³⁰	na	8.220	23.0	1.9	4.853	5.654
$\text{H}_4(\text{DPXM})$ (7)	na	6.104	16.9	26.0	4.675	4.602
$\text{Zn}_2(\text{DPX})$ ¹⁶	3.708	3.863	4.4	7.9	4.619	4.272
$\text{Zn}_2(\text{DPD})$ ¹⁷	7.775	7.587	24.6	1.2	4.800	5.577
$\text{Zn}_2(\text{DPXM})$ (8)	5.913	5.987	32.9	13.1	4.676	4.677
$\text{Mn}_2(\text{DPXM})$ (12)	5.378	4.982	20.8	19.2	4.656	4.485

^a Metrics were derived as follows. Macrocyclic centers (Ct) were calculated as the centers of the four-nitrogen (4-N) planes for each macrocycle. Interplanar angles were measured as the angle between the 4-N least-squares planes. Torsional twists were measured as the angle between the two meso-carbon to spacer bonds. The a–b and c–d separations represent the distances between the bridge carbons attached to the porphyrin meso positions and those porphyrin meso-carbons, respectively.

7. Both ring systems display a saddle conformation in the solid state. The porphyrin subunit containing N(1) to N(4) has a mean deviation from planarity of 0.23 Å with meso carbons alternately displaced from the porphyrin mean plane, ranging from 0.39 Å above to 0.38 Å below the 24-atom macrocyclic unit. The macrocycle containing N(5) to N(8) exhibits a slightly greater mean deviation from planarity (0.29 Å). Similar to the ring containing N(1) to N(4), the porphyrin with N(5) to N(8) contains meso carbons alternately displaced from the macrocyclic mean plane, ranging from 0.30 Å above to 0.36 Å below the 24-atom ring subunit. The internal pyrrolic hydrogen atoms are in their calculated positions, and are disordered over all the nitrogen atoms. An interesting feature of **7** is the small butterfly fold of the xanthene backbone along its center O(1)–C(47) axis. For **7**, the butterfly angle is 5.5°; in contrast, the parent porphyrin $\text{H}_4(\text{DPX})$ has a large butterfly distortion of 36.1°.³⁰

- (26) Fillers, J. P.; Ravichandran, K. G.; Abdalmuhdi, I.; Tulinsky, A.; Chang, C. K. *J. Am. Chem. Soc.* **1986**, *108*, 417–424.
 (27) Harvey, P. D.; Proulx, N.; Martin, G.; Drouin, M.; Nurco, D. J.; Smith, K. M.; Bolze, F.; Gros, C. P.; Guillard, R. *Inorg. Chem.* **2001**, *40*, 4134–4142.

- (28) Clement, T. E.; Nurco, D. J.; Smith, K. M. *Inorg. Chem.* **1998**, *37*, 1150–1160.
 (29) Scheidt, W. R.; Lee, Y. J. *Struct. Bonding (Berlin)* **1987**, *64*, 1–70.
 (30) Chang, C. J.; Baker, E. A.; Pistorio, B. J.; Deng, Y.; Loh, Z.-H.; Miller, S. E.; Carpenter, S. D.; Nocera, D. G. *Inorg. Chem.* **2002**, in press.

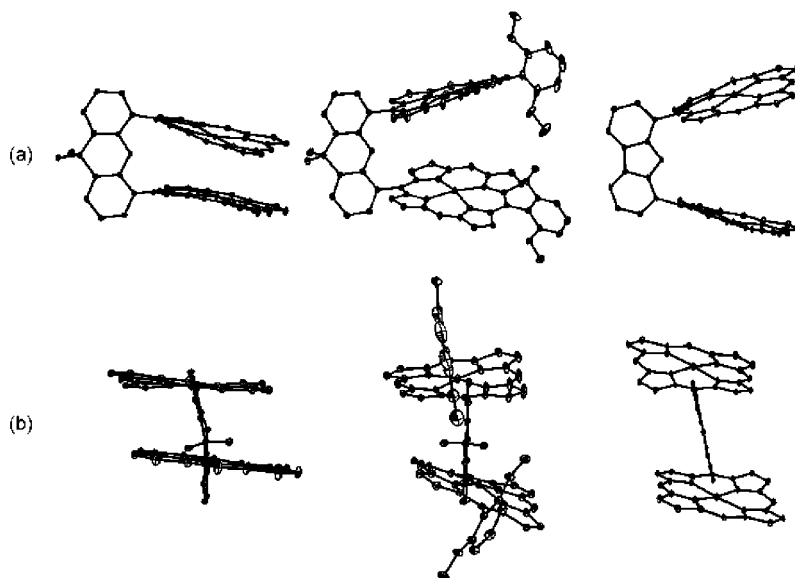


Figure 4. Comparative views of the crystal structures of $\text{Zn}_2(\text{DPX})$, **8** and $\text{Zn}_2(\text{DPD})$: (a) side view, perpendicular to the bridge plane; (b) side view, along the bridge plane. Alkyl side groups and hydrogen atoms have been omitted for clarity. Table 4 footnote defines the methods by which the crystallographically derived geometric features were measured.

8. A conformational analysis reveals inequivalent ring systems; however, both macrocycles of **8** display a saddle conformation. The core containing Zn(1) has a more pronounced saddle distortion with a mean deviation from planarity of 0.16 Å. The ring with Zn(2) has a mean deviation from planarity of 0.11 Å. The zinc(II) ions are situated in different coordination environments. Zn(1) is five-coordinate, binding an axial methanol solvate within the bisporphyrin pocket at a distance of 2.175(5) Å. The Zn(II) core adopts an approximate square-pyramidal geometry, as the N–Zn–N bond angles are $90^\circ \pm 3.5^\circ$ and the N–Zn–O bond angles are $90^\circ \pm 9.2^\circ$. The zinc center is displaced slightly from the porphyrin mean plane toward the axial ligand (0.21 Å). The average equatorial Zn–N bond length of 2.062(4) Å is in good agreement with literature values for five-coordinate zinc(II) porphyrins.³¹ In contrast, Zn(2) is six-coordinate, binding an axial methanol solvate outside the bisporphyrin pocket and an axial water molecule inside the cofacial cleft. The Zn–O bond lengths for the axial methanol and water are 2.252(6) and 2.459(17) Å, respectively. The Zn(II) center assumes a distorted octahedral geometry, and is displaced 0.11 Å toward the outer face of the bisporphyrin toward the axial methanol; the N–Zn–N bond angles are $90^\circ \pm 3.2^\circ$ and the N–Zn–O bond angles are $90^\circ \pm 5.5^\circ$. The average equatorial Zn–N bond length is 2.057(5) Å.

12. The pentacoordinate Mn centers assume a highly distorted square-pyramidal geometry, as the N–Mn–N bond angles are $90^\circ \pm 4.7^\circ$ and the N–Mn–Cl bond angles are $90^\circ \pm 10.3^\circ$. The axial chlorides are coordinated to the Mn(III) ions outside the cofacial pocket with an average Mn–Cl bond length of 2.405(2) Å. The metal centers Mn(1) and Mn(2) are displaced out of the porphyrin planes toward the axial chloride ligands by 0.25 and 0.27 Å,

respectively. The average Mn–N bond length is 2.009(5) Å. Both Mn(III) macrocycles exhibit a pronounced nonplanar distortion. The macrocycle containing Mn(1) has a mean deviation from planarity of 0.70 Å, while the ring with Mn(2) has a mean deviation from planarity of 0.64 Å.

Taken together, the crystallographic data reveal that the introduction of a single aryl group *trans* to the spacer can considerably alter the pocket sizes of pillared cofacial bisporphyrins. The molecular structures of homologous biszinc(II) complexes of the DPX, DPXM, and DPD series shown in Figure 4 confirm that this type of substitution for the DPXM framework affords a family of bisporphyrin platforms that exhibit vertical pocket sizes that are intermediate to those of the parent DPX and DPD systems. This is clearly illustrated by the observed center-to-center distances, which vary from 5.0 to 6.1 Å for the DPXM platforms. For comparison, the DPX and DPD systems have center-to-center distances of 3.8–4.7 Å and 7.6–8.2 Å, respectively. The pocket size enlargements of the DPXM series compared to their DPX counterparts are predominantly due to vertical changes, revealed by the interplanar angles between the two porphyrinic subunits. The DPXM series has interplanar angles in the range of 16.9–32.9°. In contrast, the ring-parallel DPX complexes display interplanar angles of less than 5°. Horizontal changes are modest, as the torsional angles for the structures of **7**, **8**, and **12** are all less than 26°.

Concluding Remarks

The success of cofacial bisporphyrins for efficient multielectron catalysis has traditionally relied on the choice of spacer to provide a suitable cavity for substrate activation. In contrast, our results reveal that strategic modification of the porphyrin superstructure by substitution *trans* to the spacer can also dramatically tune the vertical pocket sizes of cofacial bisporphyrins. To this end, the synthesis and

(31) Kadish, K. M.; Smith, K. M.; Guillard, R. *The Porphyrin Handbook*; Academic Press: San Diego, 2000.

coordination chemistry of methoxyaryl-modified xanthene (DPXM) and dibenzofuran (DPDM) systems has been achieved. In particular, crystallographic analysis confirms the ability of the DPXM platform to provide cofacial pockets with vertical pocket sizes that span the parent DPX and DPD platforms. The modular nature of this synthetic methodology should provide ready access to more intricate structural modifications, as the prerequisite aryldipyrrylmethanes are readily obtained in large gram-scale quantities. The application of these and related systems for the study of proton-coupled small-molecule activation is underway.

Acknowledgment. C.J.C. thanks the MIT/Merck Foundation and the National Science Foundation for predoctoral fellowships. We thank P. Landing for inspiring discussions. This work was supported by the National Institutes of Health (Grant GM 47274).

Supporting Information Available: X-ray crystallographic file (CIF). This material is available free of charge via the Internet at <http://pubs.acs.org>.

IC025507K